MATERIAL CONSTITUTIVE MODEL OF DUAL PHASE STEEL AND SPRINGBACK SIMULATION IN THE METAL FORMING APPLICATION

HARYANTI SAMEKTO
WINARDI SANI
DARWIN SEBAYANG
SULAIMAN HASAN
MUSTAFA YUSOF

This report was findings from the above stated research, carried through the Fundamental Research Grant Scheme (FRGS) vot 0369 sponsored by the Ministry of Higher Education (MOHE)

Faculty of Mechanical Engineering and Manufacturing
University Tun Hussein Onn Malaysia

DECEMBER, 2010

ABSTRACT

Applications of dual phase (DP) steel are increasing due to its excellent features; those are high tensile test and good formability. DP steel offers high ratio between strength and weight which is crucial in the performance of light weight construction, as well as capability to be deformed into complex geometry. The major disadvantage of the application of DP steel in metal forming is the occurrence of springback resulted by the elasticity recovery after load is released. The geometrical discrepancy due to springback can cause problem in part assembly and geometric deviation of the design. If springback could be predicted, the tool and die could be accurately designed and built. Many simplified analytical model have been developed to predict springback, however these model managed to cover only simple geometries. For real part geometry, finite element (FE) method should be deployed. However, the accuracy of the springback prediction is influenced by material and process parameters included in the FE analysis.

This study was focused on the investigating of the elastic-plastic behavior of DP steel following by the micro and macro modeling by using FEM. Uniaxial tensile testing was used to obtain stress and strain relationship and metallographic observation was conducted to identify phases and interaction between martensite particle and ferrite matrix during forming.

Micro mechanical FE analysis depicted that under uniaxial stress ferrite grains elongated and martensite particles were inclined to accumulate. Grain boundaries were areas with the highest strain and failures could initiate in these areas. SEM micrograph confirmed the FE analysis results. FE simulation of uniaxial tensile testing indicated that exponential based plastic constitutive material equation represented the stress strain relationship better than linear based equation.

FE simulation results for V-shape bending and U-channel shape deep drawing as well as experimental studies demonstrated the occurrence of significant springback by the forming of DP steel. By V-shape, the geometrical discrepancy was higher than by U-channel shape, because by U-channel shape the flow of material was controlled by the blank holder force. Good agreement between FE simulation and experimental results was achieved with the standard error below 10 %.

ABSTRAK

Aplikasi besi dua fasa (dual phase steel) semakin meningkat disebabkan sifat-sifatnya yang sangat baik seperti ketegangan yang tinggi dan mudah dibentuk. Besi ini menawarkan nisbah kekuatan kepada jisim yang tinggi di mana ianya sangat penting kepada prestasi pembinaan serta kemampuan untuk berubah bentuk menjadi geometri kompleks. Kekurangan utama aplikasi besi dua fasa ini adalah terjadinya 'springback' hasil daripada pemulihan elastik selepas beban dilepaskan. Perbezaan geometri yang disebabkan oleh 'springback' bukan sahaja menimbulkan masalah semasa pemasangan malah menyebabkan rekabentuk geometri yang tersisih. Jika 'springback' dapat dikenalpasti, acuan dapat direkabentuk dan dibina dengan tepat. Banyak model analitikal yang diringkaskan telah dibangunkan untuk mengenalpasti 'springback', namun model-model ini hanya dapat digunakan dalam geometri yang ringkas. Untuk geometri yang sebenarnya, kaedah unsur terhingga (FEM) harus digunakan. Namun, ketepatan dari ramalan 'springback' adalah dipengaruhi oleh parameter bahan dan proses yang dimasukkan ke dalam analisis FE.

Penelitian ujikaji ini fokus kepada kelakuan elastic-plastik besi dua fasa dan diikuti dengan pemodelan mikro dan makro dengan menggunakan FEM. Ujian ketegangan searah telah dilakukan untuk memperoleh hubungan ketegasan dan keterikan. Pemerhatian metalografi juga dijalankan untuk mengenalpasti fasa dan hubungan antara zarah martensit dan matriks ferit semasa proses pembentukan.

Analisis FE mekanikal mikro menunjukkan di bawah ketegasan searah, butiran ferit memanjang manakala zarah martensit cenderung untuk mengumpul. Sempadan butiran adalah kawasan di mana nilai keterikan yang paling tinggi dan kegagalan mudah berlaku di kawasan ini. Mikrograf SEM telah mengesahkan keputusan analisis FE ini. Simulasi FE bagi ujikaji ketegangan searah menunujukkan persamaan bahan bagi konstitutif plastik yang berdasarkan eksponen

adalah lebih baik mewakili hubungan ketegasan dan keterikan daripada persamaan berdasarkan linear.

Keputusan Simulasi FE dan experimen bagi pembengkokkan dalam bentuk V dan U telah menunjukkan kesan 'springback yang amat ketara semasa pembentukan besi dua fasa. Bagi bentuk V, perbezaan geometri adalah amat ketara berbanding bentuk U. Hal ini adalah kerana bagi bentuk U, aliran bahan adalah dikawal oleh kuasa penghempit. Kecocokan di antara keputusan simulasi dan experimen adalah di bawah 10% sisihan piawai.

CHAPTER I

INTRODUCTION

1.1 Overview

In the last decade the application of the sheet forming technology in industries has changed rapidly due to the increasing demand of geometrical complexity and high performance of the metal parts required by design. To fulfill these needs, the advanced high strength steel - dual phase steel - has been developed. The excellent features of this material are its high tensile strength and its good formability. Therefore, the use of dual phase (DP) steel is increasing, especially in automotive industry [1, 2, 3].

Dual phase (DP) steels consist of a ferritic matrix which containing a hard martensitic second phase in the form of islands or particles which is obtained by heat treatment processes. The volume fraction of hard second phases determines its strength and the soft ferrite phase gives this steel excellent ductility. In some instances, hot-rolled DP steels can have significant quantities of bainite which is required to enhance its stretching capability.

Although the application of DP steels is growing due to its remarkable high strength, excellent ductility and toughness, however, the nonlinear material properties of DP steels has not been well defined comparing to its linear material properties. Thus, it is desirable to determine and understands the plasticity of the DP steels as it is widely applied in metal forming. Better understanding of the nonlinear

material behavior of DP steels, will enable suitable process or method of deformation being selected.

1.2 Statement of Problem

Although many studies [4, 5, 6, 7] has been carried out to investigate the metallurgical aspects and to optimise the mechanical properties and formability of dual phase steel, unfortunately the material behavior under plastic deformation have not been studied sufficiently. Thus, To better understand the interaction of ferritic matrix and martensite particles which is subjected to uniaxial stress, experimental studies as well as simulation using finite element method (FEM) are carried out which is focused on elastic plastic behaviors of the two phases in micro scale. Besides that, springback analysis is also carried out on the DP steels experimentally and numerically. The springback prediction of the DP steels is essential because based on the prediction results, the tools geometry and process parameters are modified to obtain the required product shape which in the end will result in cost and time saving.

1.3 Objective

i. To conduct the uniaxial tensile test to determine the nonlinear material properties of DP steels.
ii. To observe the microstructure of the DP steels after certain percentage of plastically deformed and micro mechanical modeling of the plasticity of DP steels by using Finite Element Method.
iii. To conduct forming simulation following by springback prediction and the simulation result is verified with experimental study.

1.4 Scope of Study

i. DP steels used in this project is Docol 800DP which is supplied by Swedish Steel Manufacturer SSAB, with ultimate tensile strength 800MPa.
ii. FEM code which is used for the micro mechanical modeling of the plasticity of DP steels is ALGOR
iii. Plasticity will be investigated by using universal tensile machine
iv. Microstructure observation is carried out by using Scanning Electron Microscope (SEM).
v. Forming simulation and springback prediction are conducted by using a general purpose transient dynamic finite element code LS-Dyna.

1.5 Benefits of Study

It is expected that at the end of this research project, the result obtained will enable us have better understanding on the plasticity of DP steels and the interaction of ferritic matrix and martensite particles when subjected to uniaxial stress. Besides that, the result obtained from the numerically predicted springback of the DP steels can be used in designing the forming dies. This will not only help to save cost and time, but also to prevent failure from occurring during deformation.

CHAPTER II

LITERATURE REVIEW

2.1 Advanced High Strength Steel (AHSS)

The AHSS are characterized as having high yield strength and high work hardening rates compared to conventional steels such as mild steel. This allows for the design of thinner components while maintaining the same load bearing capability. Besides weight reduction, AHSS also have several other advantages over conventional steels. They have good fatigue performance and excellent energy absorbing properties, both of which help to improve the durability and safety performance of the final products. If the formed AHSS parts are subjected to bake hardening operations, sheet strength can increase even higher through precipitation of carbides in the matrix. Besides that, the increased of AHSS formability allows for greater part complexity, which leads to fewer individual parts and more manufacturing flexibility. Fewer parts mean less welding and weld flanges. Depending on design, the higher strength can translate into better fatigue and crash performance, while maintaining or even reducing thickness. These advantages in mechanical and material properties make AHSS very attractive especially to the automotive industry.

The principal differences between conventional High Strength Steel (HSS) and AHSS are due to their microstructures. AHSS gain their high-performance properties in strength and formability by incorporating multi-phase microstructures,

which contain martensite, bainite and/or retained austenite in quantities sufficient to produce unique mechanical properties in yield strength and ultimate tensile strength. Specific microstructures result from precise control of the chemistry or alloying elements. The yield strengths of AHSS overlap the range of strengths between HSS and UHSS as shown in Figure 2.1.

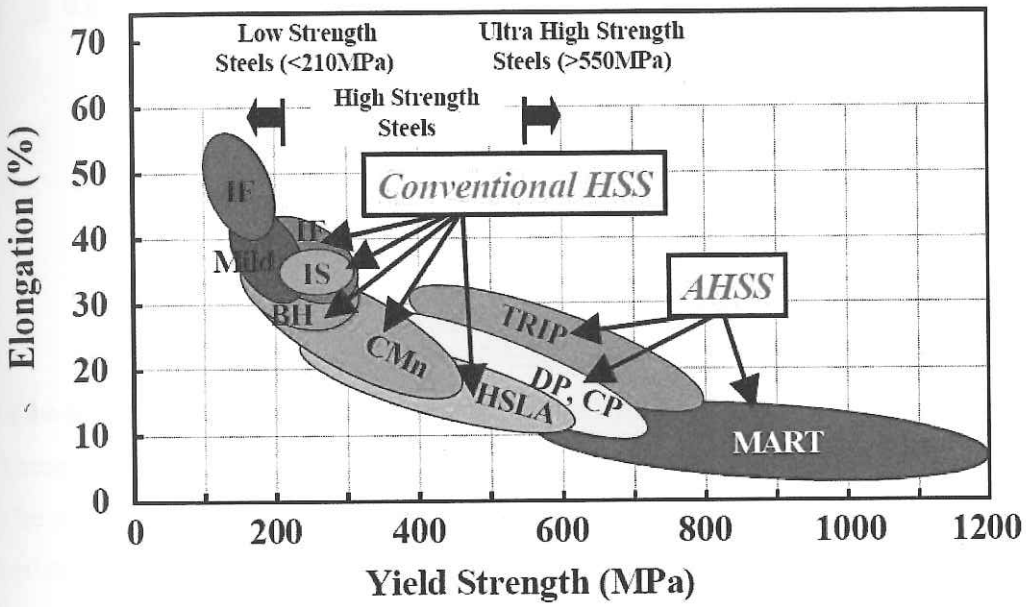

Figure 2.1: Strength – Formability relationship for conventional HSS and AHSS. [9]

Work and bake hardening also contributing to AHSS capabilities to provide these benefits, which can increase the materials' yield strength by as much as 50 percent as they undergo processing from flat sheets to complex automotive parts. The work hardening takes effect during the forming process and the bake hardening occurs as the material passes through a paint-curing process. Figure 2.2 shows the work hardening of several type of AHHS such as TRIP, DP and HSLA.

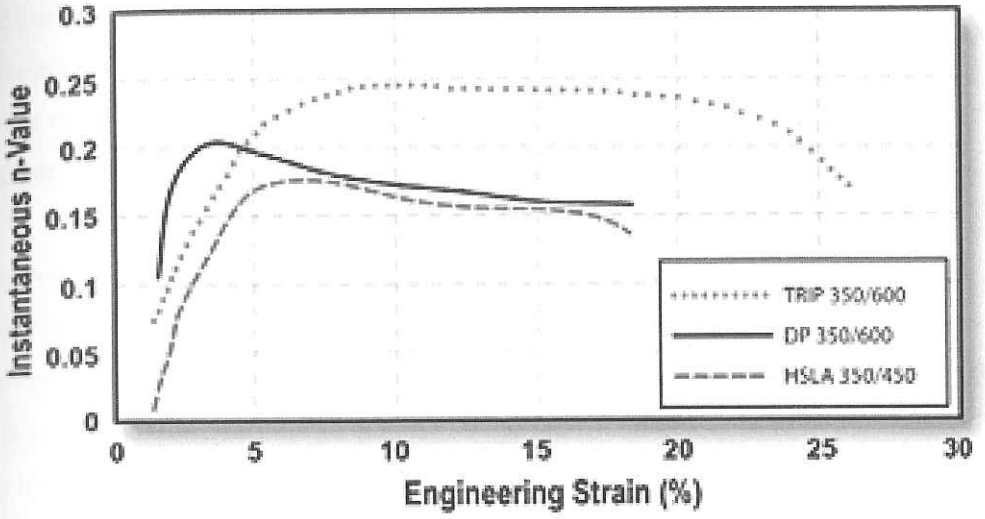

Figure 2.2: Work-hardening of HSLA, DP, and TRIP Steels [5].

There are two distinct families of steel types within the AHSS category. One is the high strength steels with increased formability for more complex part designs. These are the dual phase (DP) and transformation induced plasticity (TRIP) steels. The second family has increased tensile strength while maintaining good crush resistance and energy absorption. These are complex phase (CP) and martensitic (Mart) steels.

Dual Phase, complex phase, and TRIP steels show the most promise for automotive applications. The superior combination of strength and formability available in these steels is derived through the control of microstructure, which in the case of dual phase steels consists of ferrite and martensite, and in the case of TRIP steels ferrite, bainite and retained austenite. Alloying additions of one or more elements such as manganese, silicon, chromium, aluminum and molybdenum are necessary to develop these desired microstructures.

2.2 Dual Phase (DP) Steels

One of the main aims of steel research for automotive body applications is to develop materials with the optimum combination of relevant properties, cost, and

productivity. Dual-phase (DP) steels have demonstrated a high ultimate tensile strength (800 to 1000MPa), while maintaining a high level of ductility. Dual phase steels were developed to provide high strength formable alloys for the automobile industry to provide more flexibility in part design.

Dual phase steels consist a mixture of two phase microstructure; ferrite microstructure, with a matrix containing islands of martensite. Small amount of other phases, such as bainite, pearlite, or retained austenite, may also be present. Ferrite has a BCC crystal structure (body centered cubic) and has the advantage that it is easily formable. At the same time the good formability leads to a low strength. To increase the strength, small particles of martensite are added. This is done by a specific heat-treatment during which small particles of martensite appear. Martensite is in contrast to ferrite, is a very strong phase. But because it's very strong, it isn't good formable. A schematic representation of the microstructure of DP-steel is given in Figure 2.3.

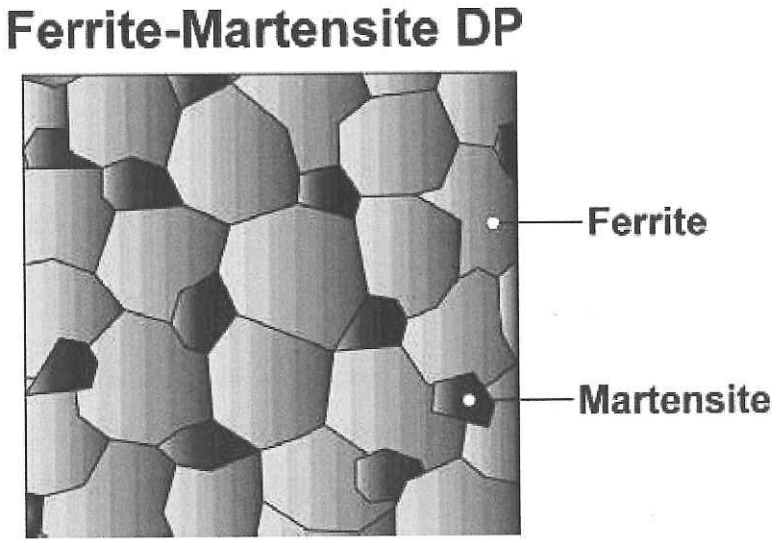

Figure 2.3: Schematic shows islands of martensite in a matrix of ferrite.

The strains related with the formation of martensite introduce free dislocations in the nearby ferrite. This gives a good combination of high tensile strength, low yield-to-tensile strength ratio and very high initial work hardening rate with good elongation values. These make the strength of the formed part to be much higher than traditional (HSLA) steel, especially at very low strain.

The unique characteristic of dual-phase steels is the continuous yielding behavior during deformation, a low 0.2% offset yield strength, and a higher total elongation than other HSLA steels of similar strength. This provides increased uniform elongation and work hardening so that those components or parts produced from dual-phase steel actually gain strength during the forming operation.

Dual Phase steels have a high initial work hardening rate, which better distributes plastic strain and improves uniform elongation. This work hardening rate will produce a much higher ultimate tensile strength than that of conventional high strength steels with similar initial yield strengths. DP steels also show a high uniform and total elongation and a lower Yield Strength / Tensile Strength ratio when compared with conventional high strength steels. These characteristics provide improvements in both formability and structural performance in automotive components. It has been applied in applications such as automobile wheel rims and wheel disks. Because of their energy-absorbing characteristics, dual-phase steels are being used in critical locations of the automobile for safety to protect the occupants in the event of a crash.

2.3 Springback

Springback is the elastically-driven change in shape of a part upon unloading after forming, is a growing concern as manufacturers increasingly rely on materials with higher strength-to-modulus ratios than the traditional low strength steel [8]. Effect of springback is that it causes the changing of the shape and dimension of the sheet metal after bending or stamping process. This has created a major problem in the assembly process. There are two terms that important in springback, namely springback controlling during forming and springback prediction in die design stage. There are many factors that could affect the springback in the process of bending or stamping, such as material variation in mechanical properties, sheet thickness, tooling geometry, processing parameters and lubricant condition [9].

Basically in springback the deformation is caused by elastic recovery. As a consequence, changes occur in the dimensions of the plastic-deformed work piece

upon removing the load. Equation 2.1 shows that the permanent deformation (ε_t) is expressed as the difference between the plastic (ε_{pl}) and the elastic (ε_e) formation.

$$\varepsilon_t = \varepsilon_{pl} - \varepsilon_e \tag{2.1}$$

When a work piece is loaded (the punch is apply to the work piece), it will have bend radius (R_i), bend angle ($\varphi_i = 180^\circ - \alpha_1$), and profile angle ($\alpha_1$) as the characteristic dimensions which is due to plastic deformation as shown in Figure 2.4.

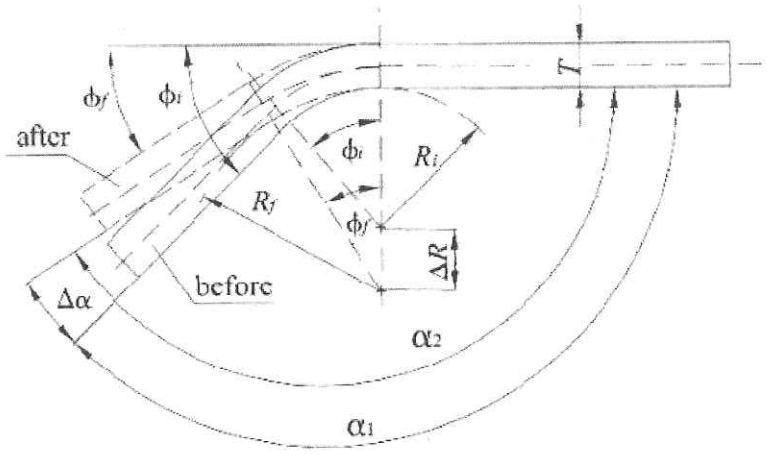

Figure 2.4: Schematic illustration of springback

The final work piece after being unloaded (the punch is removed from the work piece), there are final bend radius (R_f), final bend angle ($\varphi_f = 180^\circ - \alpha_2$), and final profile angle (α_1) [10]. The final angle after springback is smaller ($\varphi_f < \varphi_i$) and the final bend radius is larger ($R_f > R_i$) than before bending or stamping process.

There are two ways to understand and compensate for springback. One is to obtain or develop a predictive model of the amount of springback (which has been proven experimentally). The other way is to define a quantity to describe the amount of springback. A quantity characterizing springback is the springback factor (K_s) depends only on the R/T ratio, which is determined as Equation 2.2.

$$K_s = \frac{R_i + \frac{T}{2}}{R_f + \frac{T}{2}} = \frac{\frac{2R_i}{T} + 1}{\frac{2R_f}{T} + 1} = \frac{\varphi_f}{\varphi_i} = \frac{180^\circ - \alpha_2}{180^\circ - \alpha_1} \quad (2.2)$$

According to Hosford and Caddel [11], there are two conditions that happen during sheet metal bending which are tensile and compression. The moment, M that produced this bend, is calculated by assuming that there is no net external force in the x-direction ($\sum F_x = 0$). However, the internal force (dF_x) has to be considered. The relationship of the internal force is as indicated in Equation 2.3.

$$dF_x = \sigma_x w dz \quad (2.3)$$

Where σ_x is stress, w is width and is a portion of considered thickness. The change in bending moment ΔM is then being determined by using Equation 2.4;

$$\Delta M = \frac{wE't^3}{12}\left(\frac{1}{r} - \frac{1}{r'}\right) \quad (2.4)$$

Where, E' is plain strain modulus, $\Delta\sigma_x$ is unloading elastic and $\Delta\varepsilon$ is the change in strain. The elastic unloading after removal of the loads results in the residual stresses as shown in Figure 2.5.

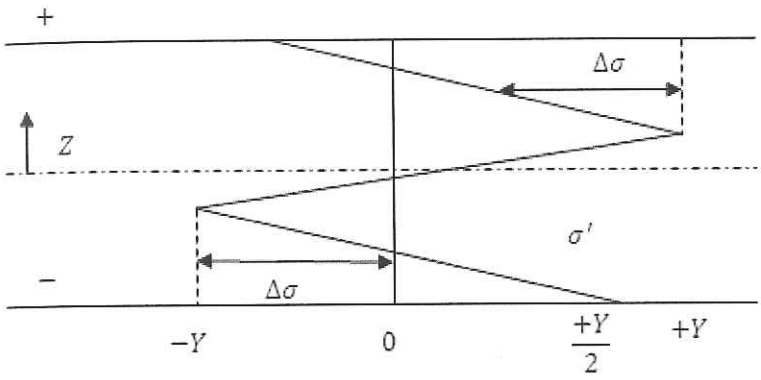

Figure 2.5: the elastic unloading after removal of the loads results in the residual stresses

While for work hardening material, if

$$\overline{\sigma} = k\overline{\varepsilon}^{n} \tag{2.5}$$

By substituting the stress, σ_x and strain, ε_x into Eq. 2.4, we get;

$$\begin{aligned} \sigma_x &= k'\varepsilon_x^n \\ &= k'\left(Z/r\right)^n \end{aligned} \tag{2.6}$$

Where

$$k' = k\left(\frac{4}{3}\right)^{\frac{n+1}{2}} \tag{2.7}$$

After the springback, $M - \Delta M = 0$;

$$\frac{1}{r} - \frac{1}{r'} = \frac{3\sigma_0}{tE'} \tag{2.8}$$

2.4 Reviews on Previous Research

S. Al Azraq et. al. [12] has studied the springback phenomenon by simulating a test case of stamping process on advanced sheet metal materials. The simulation is carried out by using the AutoForm 4.04 Incremental software code. In the research, two Advanced High Strength Steels (AHSS) with the different hardening curve are considered which are Dual-Phase 600MPa (DP 600) and Transformation-Induced Plasticity 800MPa (TRIP 800). A comparison on normal displacement in 10° profile between Dual Phase 600MPa and Transformation-Induced Plasticity 800MPa has been carried out.

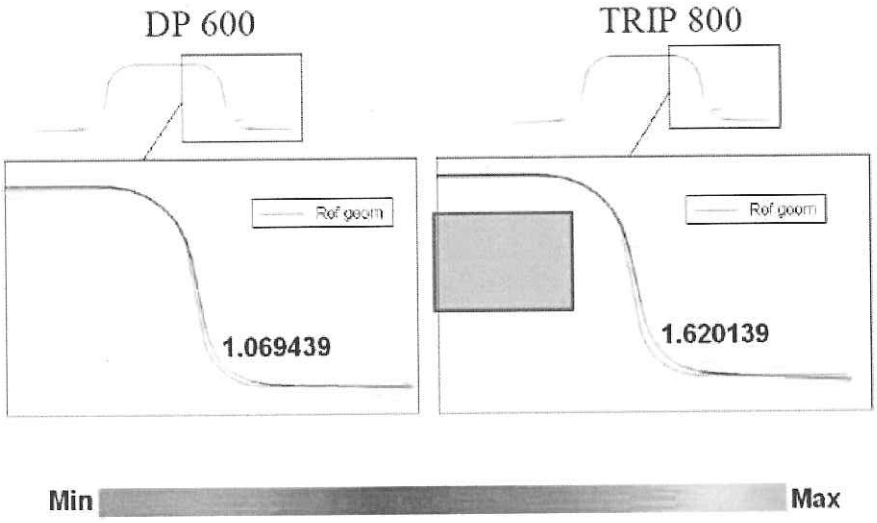

Figure 2.6: Normal displacements for different AHSS [12].

Table 2.1: Displacements for DP 600 and TRIP 800 [12].

	Displacement	DP 600	TRIP 800	Difference (%)
10°	X (mm)	0,96	1,50	56,3
	Y(mm)	0,20	0,23	15,0
	Z(mm)	0,95	0,97	2,1
	Normal(mm)	**1,07**	**1,49**	**39,3**
	Angular[°]	**4,89**	**5,06**	**3,5**
11°	X(mm)	1,04	1,63	56,7
	Y(mm)	0,22	0,26	18,2
	Z(mm)	1,20	1,06	-11,7
	Normal(mm)	**1,20**	**1,69**	**40,8**
	Angular[°]	**5,02**	**5,31**	**5,8**
12°	X(mm)	1,02	1,79	75,5
	Y(mm)	0,26	0,26	0,0
	Z(mm)	1,29	1,18	-8,5
	Normal(mm)	**1,30**	**1,93**	**48,5**
	Angular[°]	**5,20**	**5,73**	**10,2**

Figure 2.6 and Table 2.1 show the results of the normal displacement in 10° profile. For the same material, it can be conclude that the springback increases with the increasing of angular variation. For the same angle profile, it can be concluded that material TRIP 800 has more displacement than material DP 600 [12]. By using Finite Element Method, the springback can be analyzed and it shows that the analysis able to predict the influence of material strength and thus decrease the springback problem in actual parts for the future.

Finite Element Analysis of springback in L bending of sheet metal has been done by Y.E. Ling et. al. [13]. It focuses on a parametric study on how the inclusion of a step in the die may reduce springback. The outcome of this research has provided a better understanding of how die parameters like die clearance, die radius, step height and step distance (as shown in Figure 2.7) affect the springback. The material which is used in the present study is aluminum AL2024-T3 and its properties are as given Table 2.2.

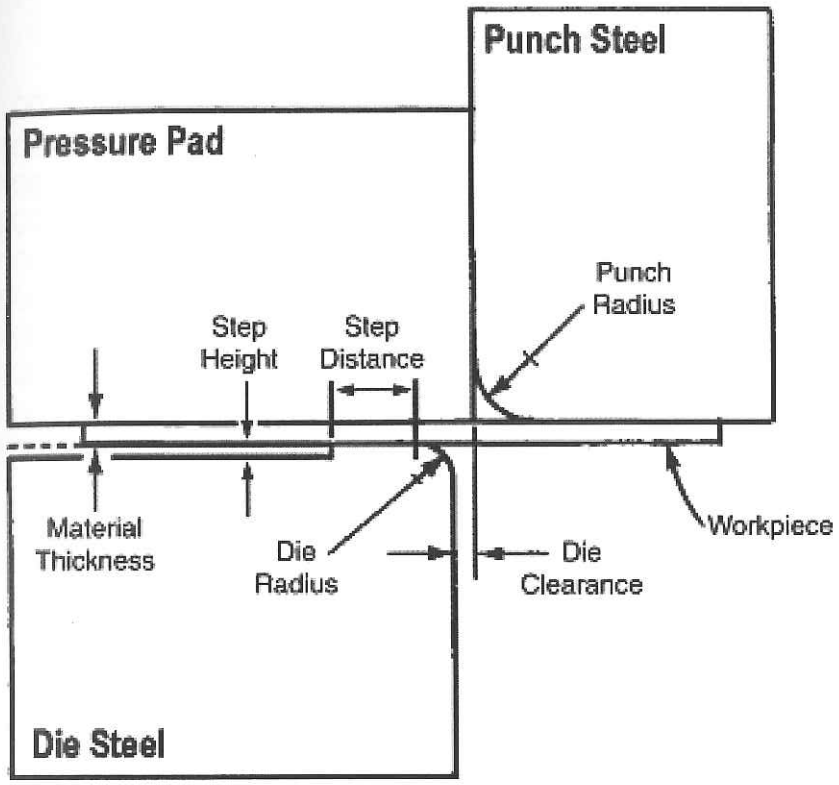

Figure 2.7: Die parameter used in this study [13].

Table 2.2: Properties of Aluminum, AL2024-T3 [13].

Modulus of elasticity ($lb/in^2 \times 10^6$)	**Poisson's ratio**	**Yield stress ($lb/in^2 \times 10^3$)**	**Ultimate stress ($lb/in^2 \times 10^3$)**	**Elongation (%)**
10.6	0.33	50	70	18

There are 5 batch of simulation listed in the present study, for the 1st batch consists of 50 simulations, 2nd batch consists of 30 total simulations, the 3rd, 4th and 5th batch same as 2nd batch which is 20 batch except for the step distance, which is changed to $1t$, $2t$, and $3t$. For the first batch, the die clearances that is used is $0.75t$, $0.80t$, $0.85t$, $0.90t$, $0.95t$, $0.98t$, $1.00t$, $1.03t$, $1.05t$ and $1.10t$ while die radii is $0.5t$, $1.0t$, $2.0t$, $3.0t$ and $4.5t$ .For the second batch which consists of simulations with step heights of $0.1t$ and $0.2t$, and step distance of $0t$. For each step height, simulations are carried out for die clearances of $0.75t$, $0.85t$, $0.95t$, $1.00t$, $1.10t$, and at die radii of $2.0t$, $3.0t$ and $4.5t$. By comparing the first batch of simulations, the values for die clearances have been reduced from 10 to 5 (Figure 2.8), and the values for die radii have been reduced from 5 to 3 [13].

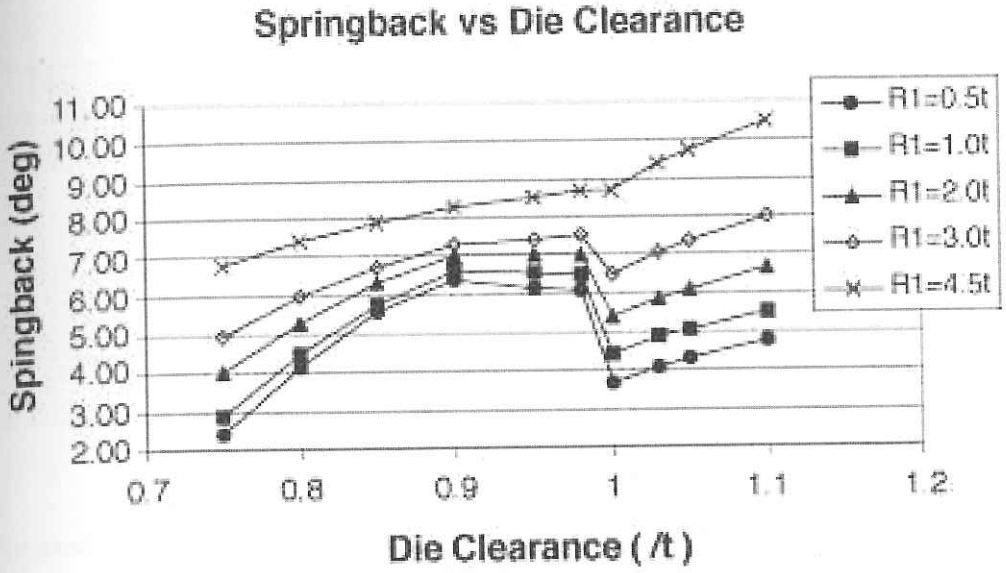

Figure 2.8: Graph of springback versus die clearance [13].

It is concluded that the parameters of die radius, clearance, step height and step distance have been used to reduce the springback. By comparing the parameters, die radius and clearance have the more significant effects on springback comparing to step height and step distance. It is recommended that to use as small die radius as possible to reduce springback. However, care must be taken to avoid using a die radius smaller than the minimum bend radius of the material. This is to prevent the bend area from cracking [13].

Table 2.3: Spring-back reduction for die clearance below 1t [13].

Die Clearance	**Springback reduction (°)**				
(/t)	**$R_1 = 0.5t$**	**$R_1 = 1.0t$**	**$R_1 = 2.0t$**	**$R_1 = 3.0t$**	**$R_1 = 4.5t$**
0.75	1.27	1.60	1.37	1.55	1.93
0.80	-	-	0.08	0.50	1.28
0.85	-	-	-	-	0.81
0.90	-	-	-	-	0.43
0.95	-	-	-	-	0.20
0.98	-	-	-	-	0.01

Table 2.4: Recommended step heights for die radius 2*t* [13].

Die clearance (/*t*)	Recommended step heights					
	Step distance = 0*t*		Step distance = 1*t*		Step distance = 2*t*	
	Step height to use (/*t*)	Springback reduction (°)	Step height to use (/*t*)	Springback reduction (°)	Step height to use (/*t*)	Springback reduction (°)
0.75	0.2	1.08	0.1	1.04	0.1	1.08
0.85	0.2	1.01	0.1	1.54	0.1	1.12
0.95	0.2	0.94	0.1	1.27	0.1	1.28
1.00	0.2	1.16	0.2	1.26	0.2	1.34
1.10	0.2	1.20	0.2	1.18	0.2	1.39

For example, consider the following configuration:

Die radius=2.0*t*; *Die* clearance=0.75*t*; *Step* height=0.2*t*; *Step* distance=0*t*.

The springback reduction for die radius 2.0*t* and die clearance 0.75*t* is 1.37° and the springback reduction for using a step height of 0.2*t* and step distance 0*t* at that die radius and clearance is 1.08°. Therefore the total springback reduction is 1.37 + 1.08 = 2.45° [13].

W. D. Carden et. al. [14] has carried out the measurement of springback. Materials that are used in the present study are DQSK steel, HSLA steel and 6022-T4 aluminum.

Material σ_y: yield stress r_{RD}: plastic anisotropy, RD	Strain	Stress equation (c = correlation coefficient)	Constants
DQSK	$\varepsilon < 0.0035$	$\sigma = E\varepsilon$	E = 212 GPa
(t = 1.50 mm)	$\varepsilon > 0.0035$	$\sigma = A[(B+\varepsilon)^C - De^{-F\varepsilon}]$	A = 539 MPa
(σ_y = 159 MPa)			B = 0.00965
(r_{RD} = 1.87)		c = 0.99983	C = 0.274
			D = 0.278
			F = 1700
HSLA	$\varepsilon < 0.0012$	$\sigma = E\varepsilon$	E = 202 GPa
(t = 1.50 mm)	$0.0012 < \varepsilon < 0.0253$	$\sigma = A[B + C\varepsilon - (1 - D\varepsilon^2)e^{-F\varepsilon}]$	A = 592 MPa
(σ_y = 414 MPa)			B = 0.686
(r_{RD} = 0.69)		c = 0.99692	C = 1.044
			D = 109000
			F = 995
	$\varepsilon > 0.0253$	$\sigma = K\varepsilon^n$	K = 772 MPa
		R = 0.99987	n = 0.163
6022-T4	$\varepsilon < 0.002$	$\sigma = E\varepsilon$	E = 69 GPa
(t = 0.91 mm)	$\varepsilon > 0.002$	$\sigma = A[1 - B\exp(-C\varepsilon) - De^{-F\varepsilon}]$	A = 389 MPa
(σ_y = 172 MPa)			B = 0.566
(r_{RD} = 0.73)		c = 0.99992	C = 8.44
			D = 1.20
			F = 1120

Figure 2.9: Material properties of DQSK steel, HSLA steel and 6022-T4 aluminum [14].

It consists of two hydraulic actuators that oriented at 90° to one another, with a fixed or rolling cylinder at the intersection of their action lines. A constant restraining force (or back force) given at the upper actuator while at the lower actuator was set to displace at a constant speed. Tensile loading, bending, and unbending are the process which the materials will undergo as it is drawn over the tooling. At the end of the test, the materials are allowed to experience springback by removing the specimen from the grips of the fixtures.

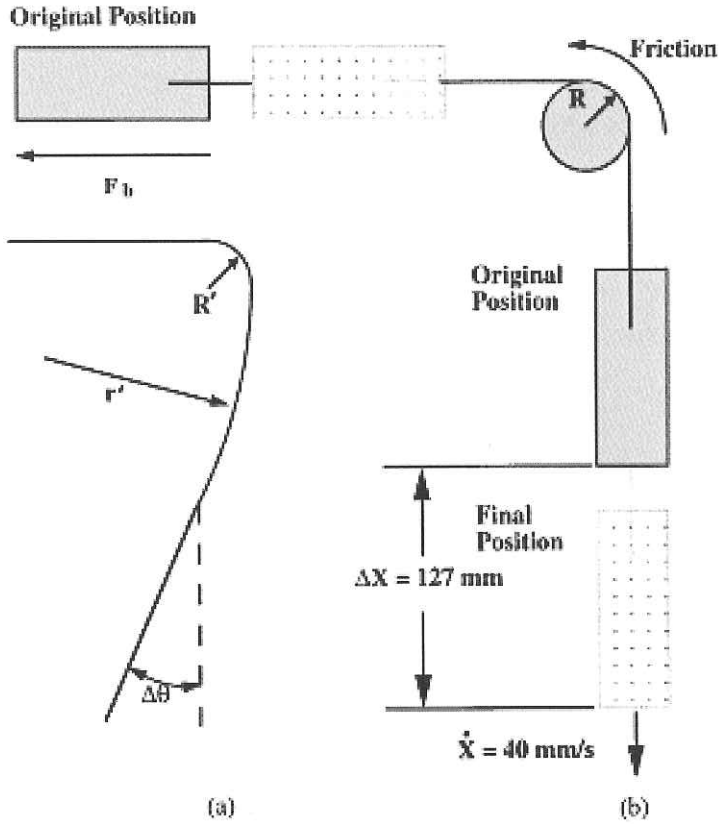

Figure.2.10: Draw/bend test geometry (a) specimen shape after unloading (b) original and final shapes during testing [14].

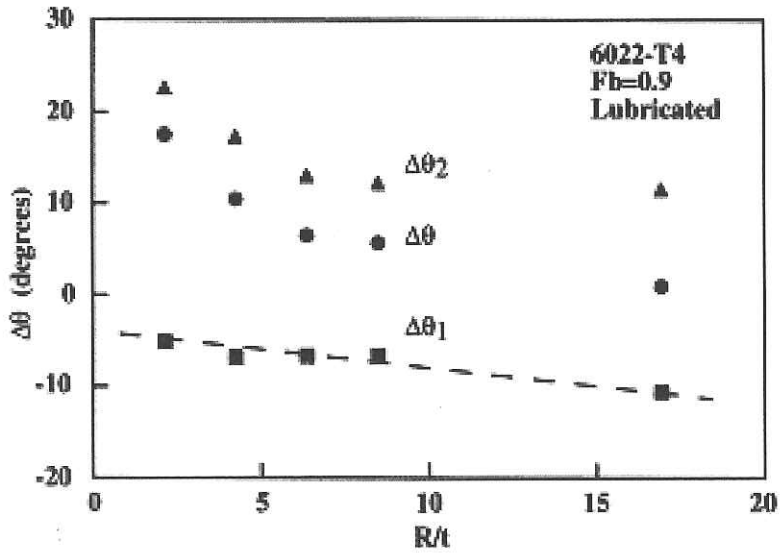

Figure.2.11: Variation of springback angle with the radius of tool-to-sheet thickness (R/t) [14].

In the result, the sheet tension had clear and dramatic effect on reducing total springback. The role of increasing R/t (for a normalized back force of 0.9) is less consistent, with a significant decrease of $\Delta\theta$ for 6022-T4 and little measurable effect for HSLA and for DQSK. Only the extreme values of R/t have a significant effect. Figure 2.12 shows the typical shapes of the unloaded strips.

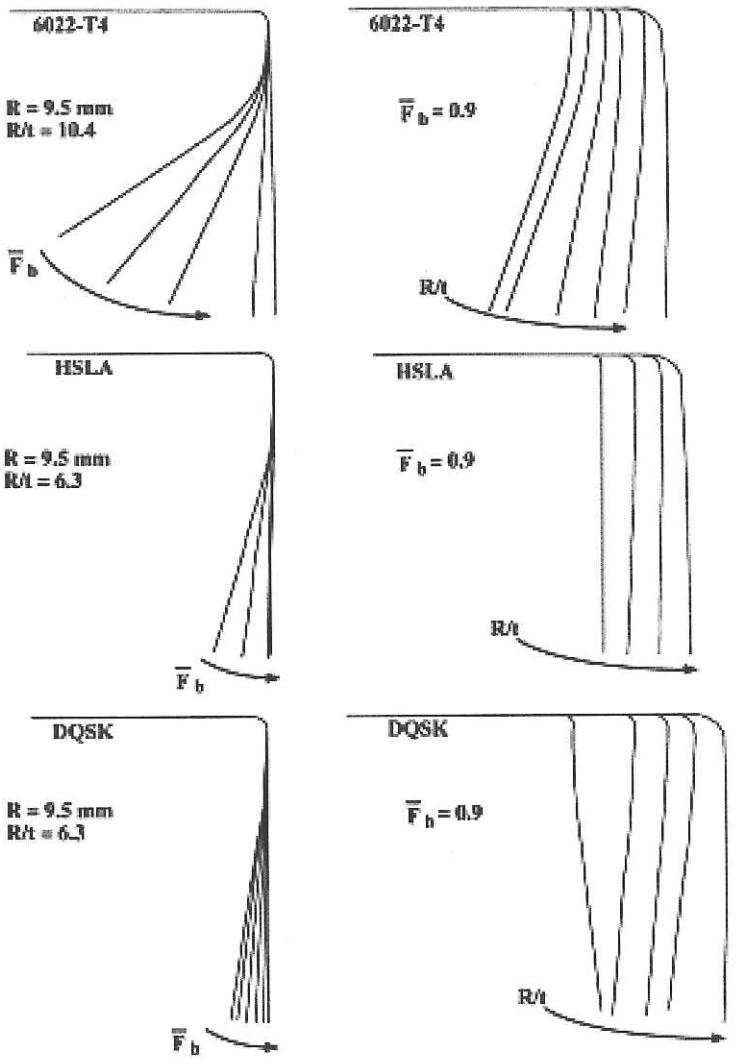

Figure 2.12: Typical final specimen shapes for variation of back force (R=9.5 m) and tool radius (F_b = 0.9) [14].

From the study, due to the extent of the affected area, the shape change associate with simple bending springback is much smaller than that associated with its dwell curl. Friction in the range normally encountered in sheet forming practice

has little effect on springback. Other than that the springback decreases for larger tool radii (R/t greater than about 5) [14].

Eggertsen P.A and K. Mattiasson [15] have carried out the constitutive modeling for springback analysis. This study has showed the importance of a correct modeling of a cyclic stress–strain behavior via a phenomenological hardening law, in order to obtain an accurate stress prediction. The main purpose of this study is to investigate the influence of two other constitutive ingredients which are the yield criterion and the material behavior during unloading. Three different yield criteria with different complexity are evaluated in the present study i.e. the Hill'48 criterion, the Barlat–Lian Yld89 criterion, and the 8-parameter criterion by Banabic/Aretz/Barlat. The springback of a simple U-bend is calculated for all the materials in the rolling, transverse and diagonal directions [15].

In this study, during unloading of the material the amount of springback depends to a great extent on the elastic stiffness of the material. In the old plasticity theory, the unloading of material after plastic deformation is assumed to be linearly elastic with the stiffness equal to Young's modulus. Thus, it is important to evaluate how the orientation of the sheet material affects the final springback of a simple U-bend problem [15].

Material	σ_0 (MPa)	σ_{45} (MPa)	σ_{90} (MPa)	σ_b (MPa)	r_0	r_{45}	r_{90}	r_b	Thickness (mm)
TKS-DP600HF	363.70	364.00	385.60	374.70	0.46	0.88	1.00	0.85	1.46
SSAB-DP600	442.20	434.10	438.60	451.11	1.03	1.07	1.15	0.90	1.00
TKS-220IF	226.70	226.10	238.90	276.98	1.60	2.10	2.42	0.96	0.96
Voest-DX56D	173.5	180.30	169.60	228.09	2.46	2.43	2.93	0.92	0.70

Figure 2.13: Material data for the steel grades and material used [15].

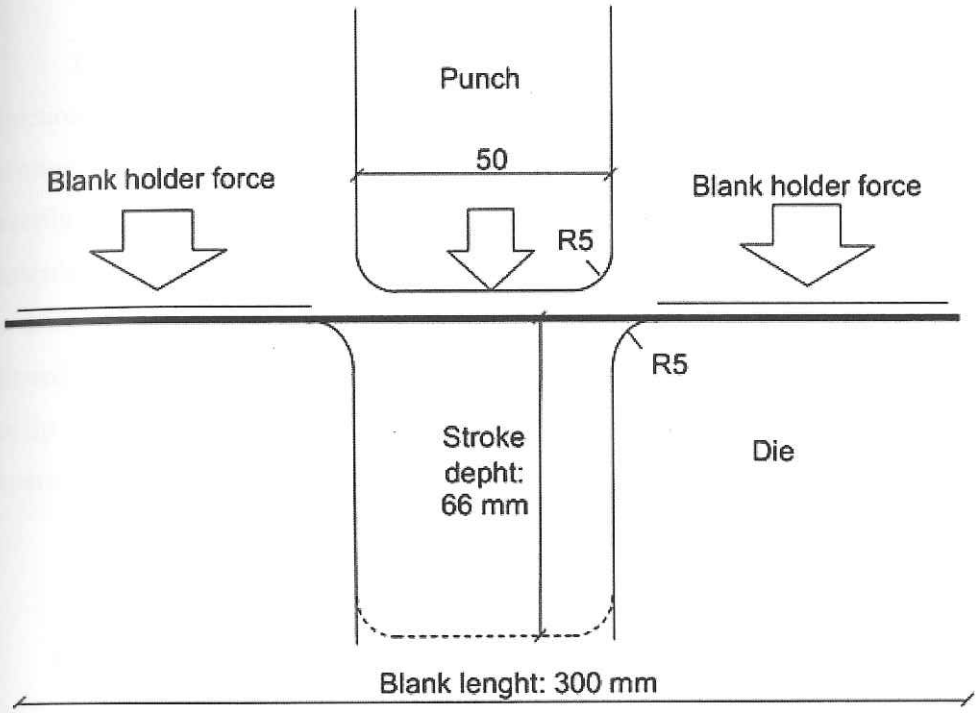

Figure 2.14: Experiment set up [15].

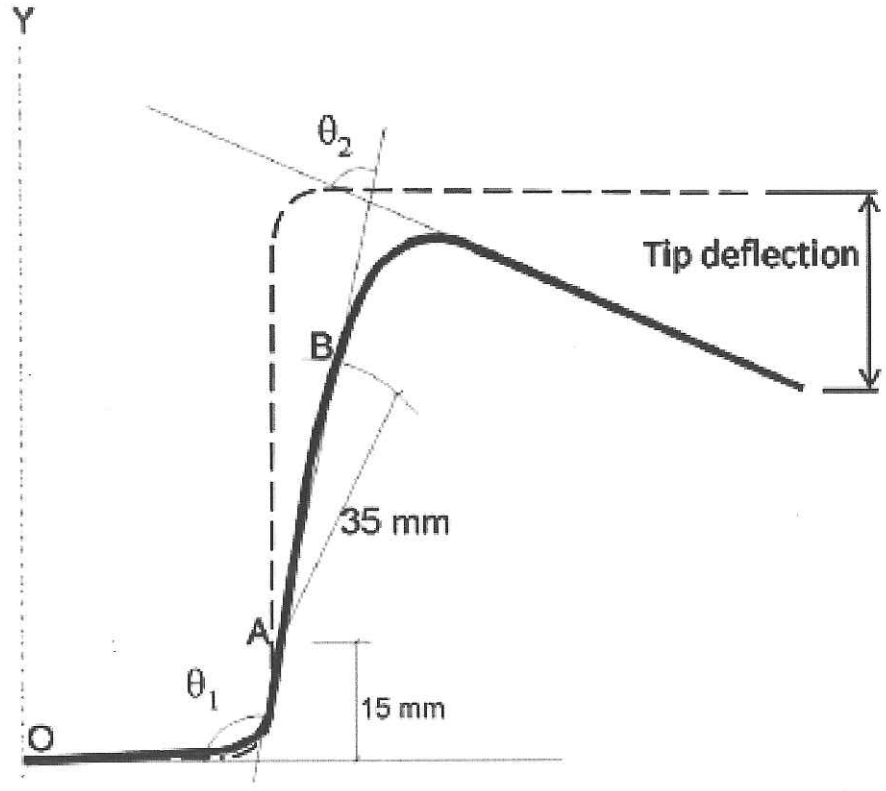

Figure 2.15: Evaluation of springback on tip deflection [15].

The springback behavior is evaluated in the rolling, transverse and diagonal directions for all four materials, and for all the three different yield criteria. It is mentioned that the Yoshida–Uemori hardening law has been proven to be best in describing the cyclic behavior. This hardening law has been used in all predictions presented in the present study. The hardening parameters in the Yoshida–Uemori hardening law is those obtained from the three-point bending test when the sheet is aligned in the rolling direction. Figure 2.16, Figure 2.17 and Figure 2.18 illustrate the tip deflections in staple diagrams and the transparent rectangular areas indicated experimental values including scatter [15].

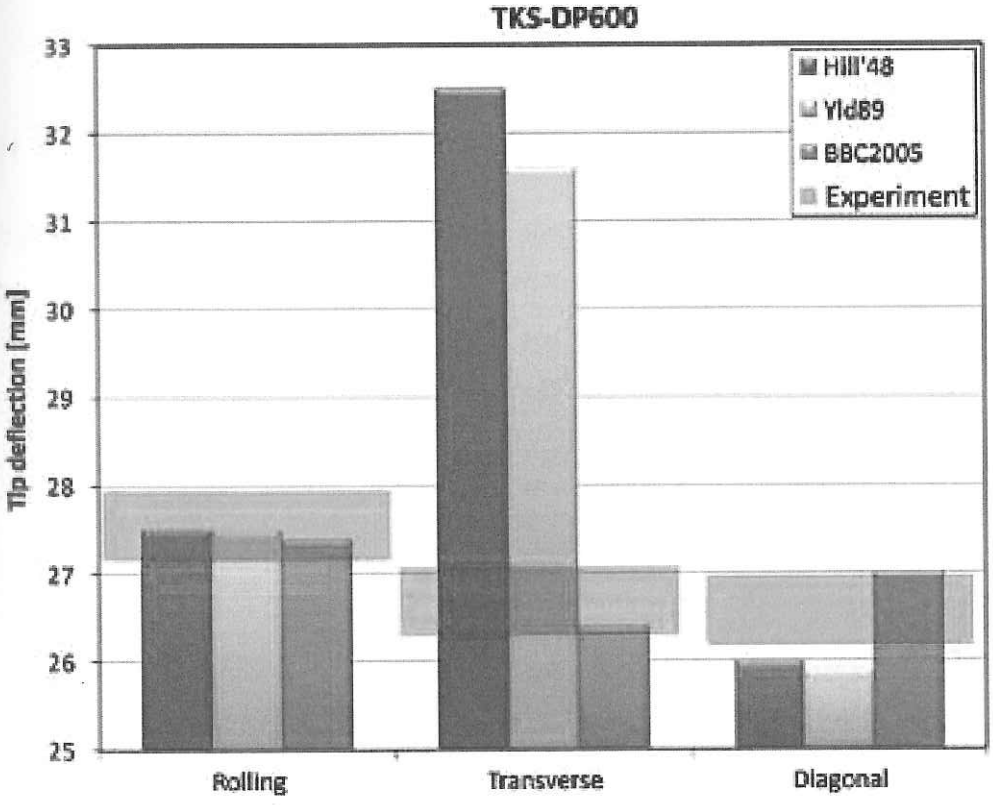

Figure 2.16: Effect of yield criterion for the springback deflection of the tip in three direction of material TKS-DP600 [15].

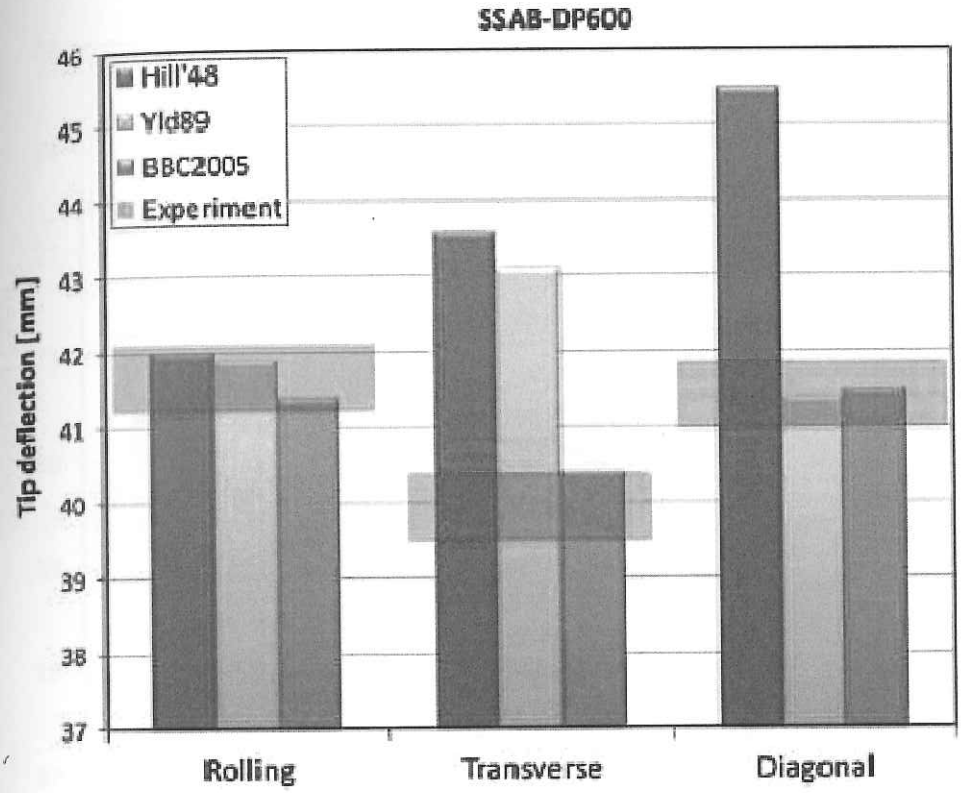

Figure 2.17: Effect of yield criterion for the springback deflection of the tip in three direction material SSAB-DP600 [15].

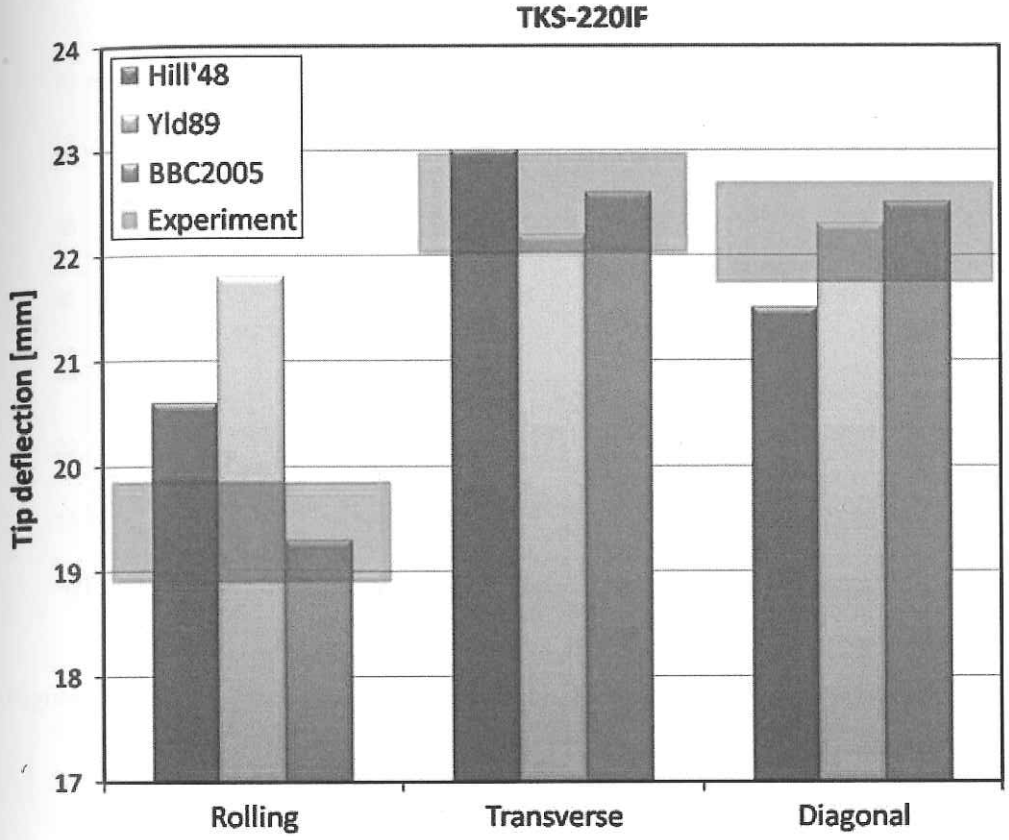

Figure 2.18: Effect of yield criterion for the springback deflection of the tip of three direction of material: TKS-220IF [15].

Base on the figures above, all the yield criteria give fairly good predictions in the rolling direction. For the other directions only the Banabic/ Aretz (BBC2005) criterion seems to give accurate springback predictions. The predictions for this criterion are inside or very close to the experimental interval for all materials and all directions [15].

In order to get accurate springback predictions, P.A Eggertsen et. al. have investigated the importance of the choice of kinematic hardening law and the importance of taking the unloading modulus into account. In the present study, the importance of the choice of yield criterion has been demonstrated. Three different yield criteria have been used to express the anisotropic behavior of the materials which are the Hill'48 yield criterion, the Barlat–Lian (Yld89) criterion and the 8-parameter yield criterion by Banabic/Aretz (BBC2005). The springback and three point bending tests are performed in the rolling, transverse, and diagonal directions for four materials which are commonly used in the automotive industry [15].